Environmental Science & Technology

Article

pubs.acs.org/est

A Mechanistic and Kinetic Study on the Formation of PBDD/Fs from PBDEs

Mohammednoor Altarawneh*,† and Bogdan Z. Dlugogorski

Priority Research Centre for Energy, Faculty of Engineering & Built Environment, The University of Newcastle, Callaghan NSW 2308, Australia

Supporting Information

ABSTRACT: This study presents a detailed mechanistic and kinetic investigation that explains the experimentally observed high yields of formation of polybrominated dibenzo-*p*-dioxins and dibenzofurans (PBDD/Fs) from the polybrominated diphenyl ethers (PBDEs), commonly deployed in brominated flame retardants (BFRs). Theoretical calculations involved the accurate meta hybrid functional of M05-2X. The previously suggested pathways of debromination and generation of bromophenols/bromophenoxys/bromobenzenes were found to be unimportant corridors for the formation of PBDD/Fs. A loss of an ortho Br or H atom from PBDEs, followed by a ring-closure reaction, is the most accessible pathway for the production of PBDFs via modest reaction barriers. The initially formed peroxy-type adduct (RO_2) is found to evolve in a complex, nevertheless very exoergic, mechanism to produce PBDDs. Results indicate that, degree and pattern of bromination, in the vicinity of the ether oxygen bridge, has a minor influence on governing mechanisms and that even fully brominated isomers of BFRs are capable of forming PBDD/Fs. We thoroughly discuss bimolecular reactions of PBDEs with Br and H, as well as the Br-displacement reaction by triplet oxygen. The rate of the Br-displacement reaction significantly exceeds that of the unimolecular inititiation reactions due to loss of ortho Br or H. Results presented herein address conclusively the intriguing question of how PBDEs form PBDD/Fs, a matter that has been in the center of much debate among environmental chemists.

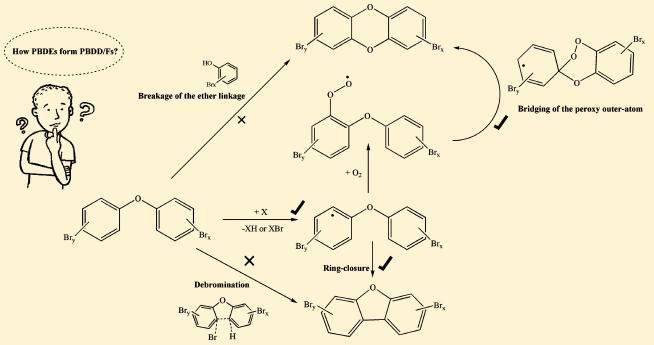

1. INTRODUCTION

Brominated flame retardants (BFRs) are a group of brominated aromatic chemicals that have the potential to significantly reduce the flammability tendency of treated objects. During the last three decades, BFRs have been widely incorporated into various consumers' products, such as electronic devices, plastics, and carpets. Polybrominated diphenyl ethers (PBDEs) are the most commonly deployed BFRs.[1] As persistent organic pollutants (POPs), PBDEs resist degradation and tend to bioaccumulate in living tissues.[2,3] Accordingly, elevated concentrations of PBDEs are being detected worldwide in various environmental matrices, both in urban and remote areas alike.[4−6] PBDEs leach to the environment throughout the life cycle of treated objects, especially as dust in the case of indoor exposure from BFRs-containing articles.[7,8] However, the major sources for the emission of PBDEs are incineration and open burning of household wastes, such as electronic parts, paints, solvents, and textiles.[9,10] As many countries deploy waste-to-energy incineration as a mainstream practice in treating municipal solid wastes,[11] emission of PBDEs into the surroundings from inadequately controlled incineration processes may add to the environmental load of PBDEs in the foreseen future. Mechanical recycling of plastics and metals also contributes significantly to the environmental burden of PBDEs.[12]

While PBDEs are toxic in their own right, they also act as potent precursors for the formation of polybrominated dibenzo-*p*-dioxins and dibenzofurans (PBDD/Fs), i.e., a group of chemicals that share similar notorious behavior with their chlorinated counterparts (PCDD/Fs).[13,14] The potency of PBDEs to form PBDD/Fs prompted the scientific community to re-evaluate their merits as flame retardants and resulted in ceasing the production and deployment of most isomers of PBDEs.[15,16] However, the decaPBDE (BDE-209) isomer in particular is still being marketed excessively[17] and PBDEs-containing articles will sooner or later be processed in municipal waste incinerators or recycling facilities, or disposed in open burning or unwanted fires. Numerous experimental studies have established inventories of the emission of PBDD/Fs from incineration of PBDEs-containing fuels, such as combustible fraction of residential waste, electronic waste, and discarded plastic resins.[18−24]

Received: December 11, 2012
Revised: March 24, 2013
Accepted: April 11, 2013
Published: April 11, 2013

Several investigators examined formation of PBDD/Fs from PBDEs. The pioneering work of Buser[25] demonstrated that thermolysis of PBDEs produces substantial quantities of PBDD/Fs, up to a maximum yield of 10%. Considerable concentrations of PBDD/Fs were consistently detected from combustion and pyrolysis of PBDEs.[22,26−30] Despite these efforts, chemical phenomena governing generation of PBDD/Fs from PBDEs are still open to great speculations. Correlations between concentrations of PBDD/Fs and PCDD/Fs in many laboratory studies and full-scale experiments[20,21,31] suggested that, the well-established mechanisms for the formation of the latter could also be responsible for the formation of the former. PCDD/Fs form along two general pathways, viz., homogeneous condensations of gas-phase precursors such as chlorophenols and chlorobenzenes (∼400−700 °C), and surface-mediated reactions, including the so-called "de novo" synthesis from a carbonaceous matrix and the catalytically assisted coupling of precursors (∼200−400 °C).[32]

Guided by experimental results, Weber and Kuch[33] reviewed mechanisms pertinent to the generation of PBDD/Fs from PBDEs. The authors demonstrated that, the potential to form PBDD/Fs depends on the operational conditions, namely, pyrolysis, open burning, controlled combustion, and thermal stress. Synthesis of PBDFs from PBDEs was suggested to proceed via a simple intramolecular elimination of HBr (i.e., debromination), and, to a much lesser extent, Br_2. It follows that the presence of a hydrogen atom in an ortho-substituted position is a prerequisite for the direct conversion of PBDDs into PBDFs. This proposed mechanism provided an explanation for the formation of lower brominated PBDFs from higher brominated PBDEs.

Suggested pathways for the formation of PBDDs from PBDEs involve oxygen insertion into PBDEs,[34] conversion of PBDEs into hydroxylated PBDEs,[35,36] and degradation of PBDEs into polybrominated phenols and benzenes.[37] Perhaps the most discussed mechanism for the formation of PBDD/Fs is the gas-phase condensation of bromophenols.[38] Experimental[39−41] and theoretical[42] studies revealed that bromophenols could form PBDD/Fs in steps analogous to those involved in the homogeneous production of PCDD/Fs from chlorophenols. In fact, bromophenols generate more PBDD/Fs than chlorophenols form PCDD/Fs at a lower onset temperature.[39,40] However, the role of bromophenols as potent precursors in the formation of PBDD/Fs from PCDEs is still not clear. PBDD/Fs were found to form at a relatively low temperature before the formation of bromophenols.[33] The presence of two ether oxygen bridges in molecules of PBDD suggests that, the source of some PBDD/Fs is likely to be the initial decomposition of PBDEs at lower temperatures (<600 °C) prior to the formation of bromophenols/bromophenoxys at temperatures of around 700 °C.

This paper reports detailed mechanistic and kinetic investigation into the formation of PBDD/Fs from oxidation of PBDEs utilizing very accurate quantum chemical calculations. The primary aim is to provide a conclusive answer to the intriguing question of how PBDEs form PBDD/Fs. The relative importance of competing reaction channels is evaluated based on their calculated reaction rate constants.

2. COMPUTATIONAL DETAILS

Structural optimization and energy calculations were carried out with use of the Gaussian 09[43] program at the M05-2X/6-311+G(d,p) level of theory. M05-2X[44] is a hybrid meta exchange correlation functional that was found to predict well the thermochemical and thermokinetic properties of chemical species, although, for specific systems, it can be outperformed by B2PLYP, M06-2X, M06, M08, M1 and other functionals. When developed, the applicability of the M05-2X functional was tested against several experimental and theoretical databases. These databases included energies of reactions involving radicals, bond dissociation energies for carbon−carbon and carbon−X (X = CH_3, H, and OCH_3) bonds, and atomization energies of open shell species. The results of this validation indicate that, the M05-2X functional can provide accurate results for systems comprising open shell radical species. To further increase the accuracy of calculations, single point energies for all structures were performed at the extended basis set of GTLarge.[45]

It is well-documented that, energies obtained from the M05 functional are very sensitive to the choice of employed quadrature grid. Wheeler and Houk[46] traced this sensitivity, in the case of the M05-2X functional, to the enhancement factor of the kinetic energy density. Accordingly, all calculations herein were carried out with use of an adequate integration grid that spans 99 and 590 radial and angular points, respectively. Calculated reaction energies for three selected reactions were found to change by only 0.005−0.002 kcal/mol, when applying a higher grid density of 120 radial points and 770 angular points. This confirms that, energies obtained from the M05-2X functional are converged with respect to the integration grid and that the grid errors are minimized. In many cases, transition structures were confirmed by calculating the intrinsic reaction coordinates (IRC).

Reaction rate constants were obtained with the aid of ChemRate according to the transition state theory (TST).[47] Contribution from tunnelling effects was incorporated in the calculated reaction rate constants based on Wigner's formula.[48] While the TST remains a popular and reliable methodology for estimating reaction rate constants for general applications, it should be noted that, for many reactions, the TST fails to account accurately for reaction rate constants and product ratios. The pioneering work by the groups of Singleton[49] and Houk[50] has demonstrated that, detailed dynamic trajectories provide a robust framework for describing many reactions. Common examples comprise regioselective and degenerate arrangements. Dynamic effects influence the topology of reaction surfaces rather than their energetics. Dynamic effects on pathways of formation of PBDD/Fs will be investigated in due course.

3. RESULTS AND DISCUSSION

A 2,2′-dibromodiphenyl ether (2,2′-DBDE) molecule is chosen as a model compound to represent PBDEs. The choice of 2,2′-DBDE stems from the fact that it contains both bromine and hydrogen substituents at the two phenyl rings. This in turn allows addressing the effect induced by atomic-type substitution on prominent reaction steps. All energetic values discussed herein are at 0 K. To enable derivation of relevant thermochemical parameters at elevated temperatures, NASA polynomials[51] are given in the Supporting Information for all species, together with their structural parameters. Modified Arrhenius parameters for all considered reactions are listed in Table 1, as fitted in the wide temperature range of 300−2000 K at the high-pressure limit. To alleviate complexity germane to

Table 1. Fitted Arrhenius Parameters (temperature range 300−2000 K) for Major Reactions in the Formation of DF, 4-MBDF, DD, and 1-MBDD from Oxidation of 2,2′-DBDE

reaction	A (s^{-1} or $cm^3 \cdot molecule^{-1} \cdot s^{-1}$)	n	E_a/R (1/K)
M1 → M4	3.02×10^{10}	0.21	8 200
M1 → M6	9.55×10^{10}	0.36	22 300
M1 → M8	9.33×10^{11}	0.26	12 900
M7 → M14	6.03×10^{11}	0.53	27 900
M7 → M13	2.24×10^{10}	0.04	11 500
M7 → M12	6.31×10^{10}	0.19	13 300
M4 → M5	2.29×10^{12}	0.24	7 500
M5 → M9	1.66×10^{11}	0.13	10 200
M5 → M10	2.27×10^{12}	1.08	14 600
M5 → M11	1.66×10^{10}	0.72	15 100
M11 → M10	2.34×10^{11}	0.07	12 600
M2 → M3	1.66×10^{11}	0.13	5 200
M2 → **DF** + Br	7.59×10^{11}	0.27	7 500
M3 → H + **4-MBDF**	5.25×10^{10}	0.81	10 300
M13 → H + **1-MBDD**	4.68×10^{10}	0.97	14 900
M4 → M17	2.29×10^{13}	−0.14	7 000
M17 → M18	1.00×10^{12}	−0.29	12 100
M20 → Br + M19	1.02×10^{14}	−0.06	10 400
M20 → OBr + **DD**	4.07×10^{13}	0.05	7 500
2,2′-DBDE → Br + M2	1.50×10^{13}	0.00	41 500
2,2′-DBDE → HBr + **4-MBDF**	3.47×10^{10}	0.38	40 800
2,2′-DBDE → 2-BrPhy +2-BrPhx	3.16×10^{15}	0.00	40 200
2,2′-DBDE → Br_2 + **DF**	8.51×10^{9}	0.51	49 500
$O_2{}^3\Sigma_g$ + 2,2′-DBDE → Br + M1	3.02×10^{-23}	2.79	19 000
Br + 2,2′-DBDE → 1,2-DBrBz + 2-BrPhx	1.03×10^{-19}	1.98	8 600
Br + 2,2′-DBDE→ HBr + M21	2.51×10^{-19}	2.64	11 800
H + 2,2′-DBDE → HBr + M2	8.32×10^{-16}	1.52	4 600
H + 2,2′-DBDE→ H_2 + M21	1.82×10^{-16}	1.91	8 100
H + 2,2′-DBDE → M22	1.81×10^{-17}	1.40	4 900
H + 2,2′-DBDE→ M25	1.65×10^{-17}	1.32	3 700
H + 2,2′-DBDE→ M26	1.78×10^{-17}	1.35	3 600
H + 2,2′-DBDE→ M23	1.70×10^{-17}	1.43	3 500
H + 2,2′-DBDE→ M24	7.08×10^{-17}	1.39	4 700

nomenclature of brominated organic molecules, structures are labeled with symbols throughout the discussion.

Initial Decomposition of 2,2′-DBDE. Figure 1 depicts the reaction progress for the unimolecular decomposition of a 2,2′-DBDE molecule. Barrierless fissions of the ortho C−H, ortho C−Br, and C−O bonds are found to be endoergic by 112.1, 83.0, and 80.5 kcal/mol, respectively. Bond dissociation energies of C−H and C−Br at meta and para positions are found to differ from analogous values for ortho positions by only 0.4−1.1 kcal/mol. Hence, kinetic and thermochemical data obtained for ortho C−H and ortho C−Br should also represent corresponding values for the other two positions throughout the discussion.

By adopting A-factors from the C_6H_5-Br[52] and $C_6H_5-OC_6H_5$[53] systems, rate constants for C−Br and C−O bond fissions can be assigned expressions, as given in Table 1. Direct elimination of HBr and Br_2 molecules and the subsequent formation of 4-monobromodibenzofuran (4-MBDF) and dibenzofuran (DF) molecules are encountered with sizable reaction energies of 81.2 (TS_U1) and 98.8 kcal/mol (TS_U2), respectively. Examining rate constants in Table 1 reveals that, the rupture of the ether oxygen linkage predominates the unimolecular decomposition of the 2,2′-DBDE molecule at all temperatures. This observation concurs with early interpretation of experimental findings on the importance of the degradation of PBDEs into brominated phenols and benzenes.[54] However, the breakage of the ether linkage is too slow to form appreciable concentrations of bromophenols/bromophenoxys/bromobenzens that would sequentially act as building blocks for the formation of PBDD/Fs. Most importantly, calculations reveal that direct intramolecular elimination of HBr from PBDEs is a rather negligible corridor for the formation of PBDFs.

Bimolecular Reaction of 2,2′-DBDE with H, Br, and $O_2{}^3\Sigma_g$. *Reaction with H Atoms.* In BFRs, PBDEs are employed as miscible constituents in treated objects such as plastics. Incidentally, polymeric matrices forming these objects serve as efficient donors of hydrogen atoms. Experiments on copyrolysis of PBDEs with polymeric additives show consistent increase in the total yield of PBDDs/Fs and shifting homologue patterns toward lower brominated congeners.[55,56] The presence of a polymeric matrix also decreases the optimum temperature window for the formation of PBDD/Fs. In this respect, reaction of H atoms with PBDEs is very relevant to the synthesis of PBDD/Fs from PBDEs.

Figure 2a depicts reaction coordinates for all plausible reactions of an H atom with a 2,2′-DBDE molecule. Abstraction of an H atom is the least preferred pathway with activation energy of 17.1 kcal/mol. Figure S1 of the Supporting Information plots the branching ratio up to 0.15 to magnify the trends observed for the six bottom curves of Figure 2a. On the

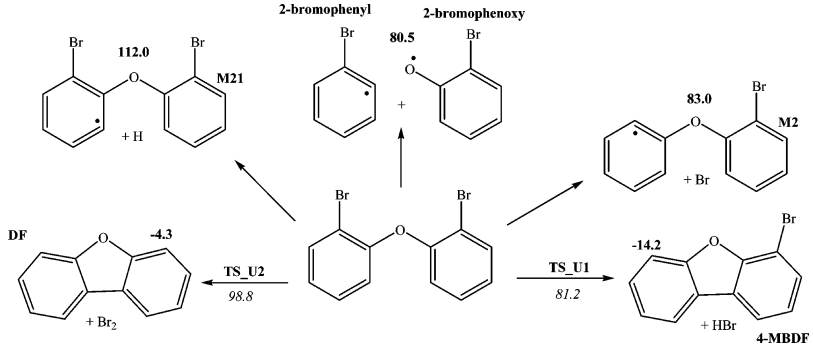

Figure 1. Reaction coordinates for pathways involved in the unimolecular decomposition of 2,2′-DBDE. Values (kcal/mol) in bold and italic are reaction and activation zero point energies, respectively, at 0 K. Values are calculated at the M05-2X/GTLarge//M05-2X/6-311+G(d,p) level of theory.

dx.doi.org/10.1021/es305081j | Environ. Sci. Technol. 2013, 47, 5118−5127

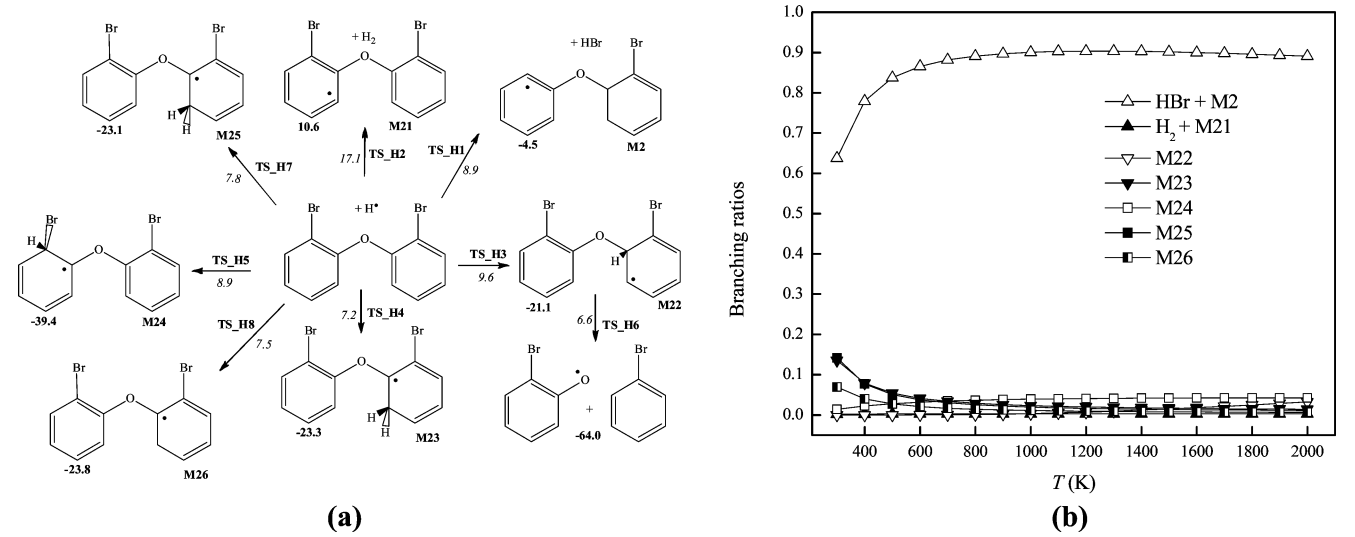

Figure 2. (a) Reaction coordinates for bimolecular reactions of H atoms with the 2,2′-DBDE molecule. Values (kcal/mol) in bold and italic are reaction and activation zero point energies; respectively (at 0 K). Values are calculated at the M05-2X/GTLarge//M05-2X/6-311+G(d,p) level of theory. (b) Branching ratios as a function of temperature for H + 2,2′-DBDE. Branching ratios are given per one abstractable/addition site for all channels. Part a is provided on a smaller scale in the Supporting Information (Figure S1).

Scheme 1

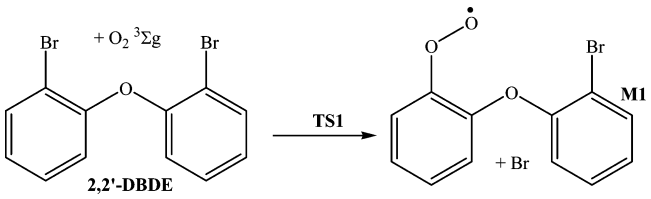

other hand, activation energy for abstraction of a bromine atom amounts to only 8.9 kcal/mol, through the transition structure of TS_H1. Barriers for addition at the three distinct sites in the 2,2′-DBDE are comparable and in the range of 7.2−9.6 kcal/mol, with structure M23 representing the addition at nonbrominated sites 3 to 6 of a 2,2′-DBDE molecule. Addition at the pivot carbon atom affords structure M22 accompanied by an exoergicity of 21.1 kcal/mol. The position of an H atom at the ether bridge facilitates its rupture via a trivial barrier of 6.6 kcal/mol. Formation of 2-bromophenoxy and bromobenzene is highly exoergic by 64.0 kcal/mol. To evaluate the relative importance of the five available channels, their branching ratios are plotted in Figure 2b, based on their calculated rate constants that are listed in Table 1. To allow the results to be extended to all PBDEs in general, without complications due to the number of available brominated and nonbrominated sites, branching ratios are given per one abstractable/addition site for all channels. Abstraction of a bromine atom is found to be the sole important channel at all temperatures. This finding is in accord with experimental observations. For instance, Luijk et al.[56] reported a wide range of lower brominated congeners of PBDEs upon cothermolysis/pyrolysis of decaBDE emplaced in typical polymeric matrices. High selectivity of hydrogen atoms to abstract bromine atoms also underpins shifting the homologue profile of PBDD/Fs to lower brominated congeners, as evident in many experimental studies. As only highly brominated PBDEs are typically employed as modern

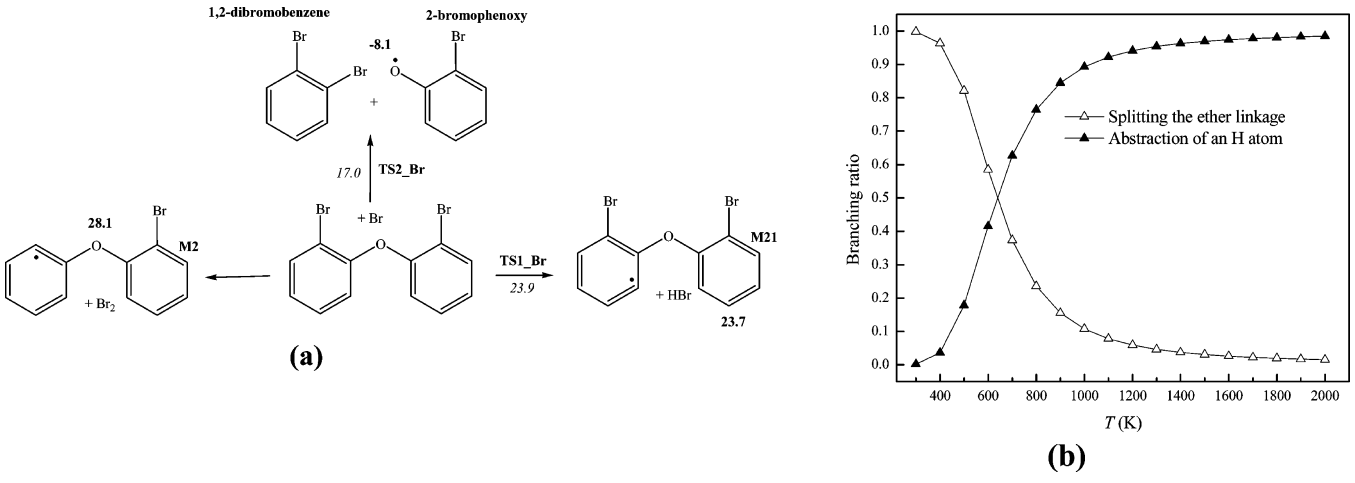

Figure 3. (a) Reaction coordinates for bimolecular reactions of Br atoms with the 2,2′-DBDE molecule. Values (kcal/mol) in bold and italic are reaction and activation zero point energies; respectively (at 0 K). Values are calculated at the M05-2X/GTLarge//M05-2X/6-311+G(d,p) level of theory. (b) Branching ratios as a function of temperature for Br + 2,2′-DBDE.

dx.doi.org/10.1021/es305081j | Environ. Sci. Technol. 2013, 47, 5118−5127

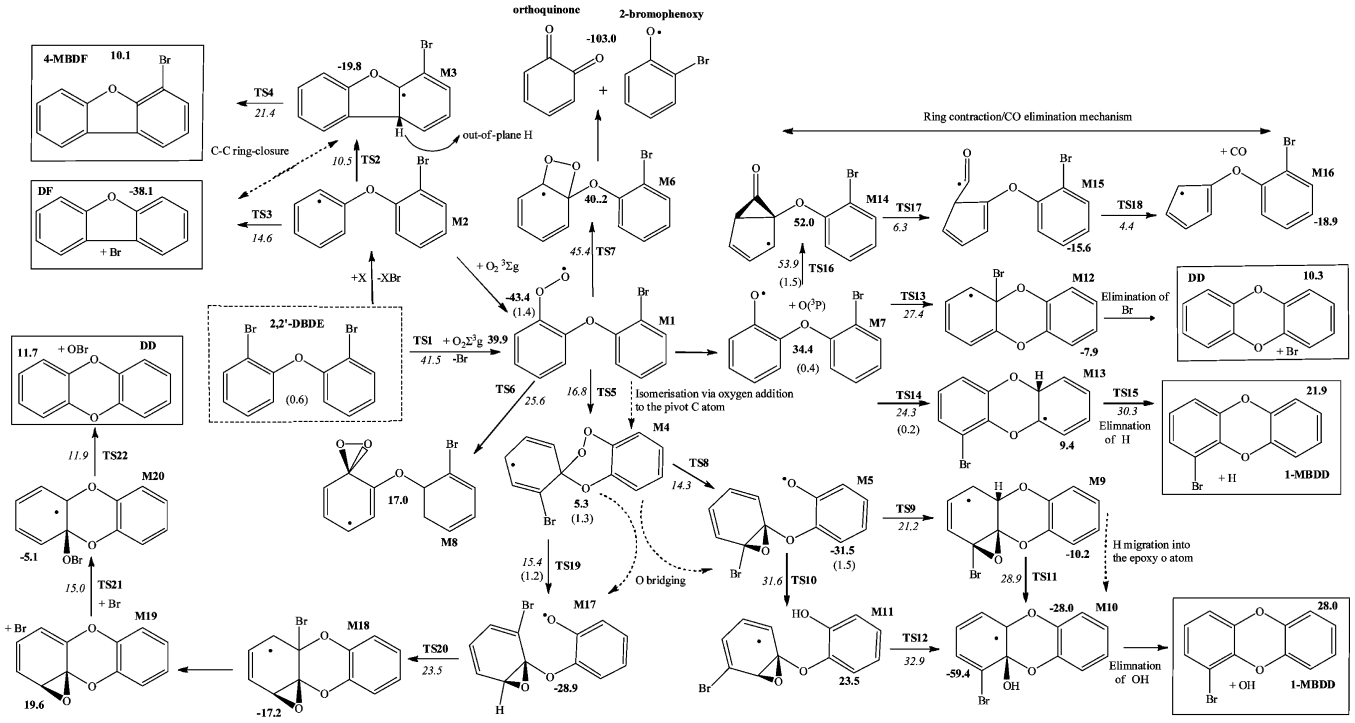

Figure 4. Formation of DF, 4-MBDF, DD, and 1-MBDD from oxidation of 2,2′-DBDE. Values (kcal/mol) in bold and italic are reaction and activation zero point energies, respectively (at 0 K). Values are calculated at the M05-2X/GTLarge//M05-2X/6-311+G(d,p) level of theory. Difference in energies between plausible conformers are given in parentheses.

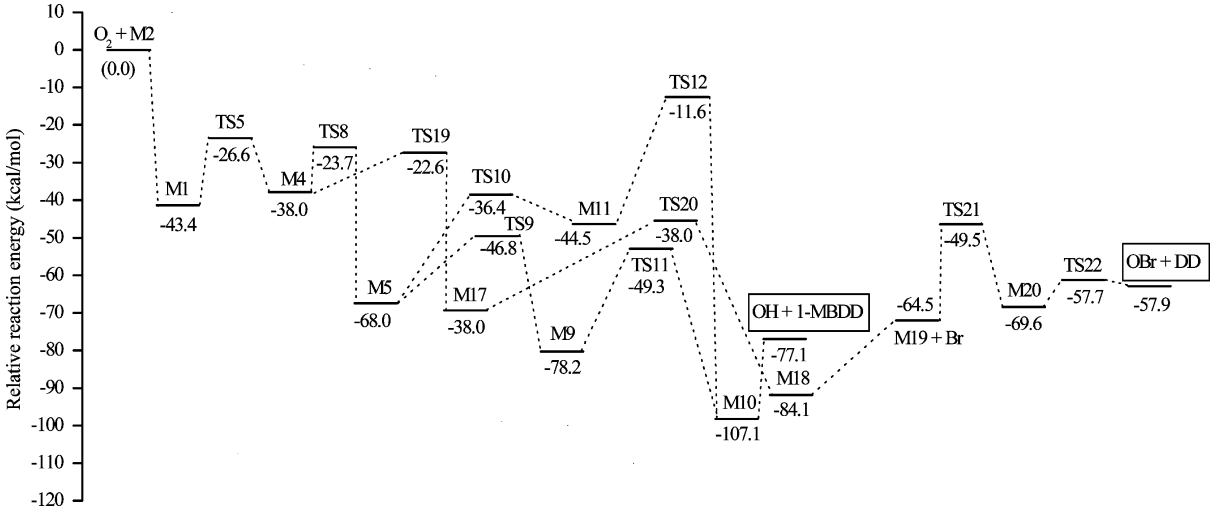

Figure 5. Relative reaction coordinates for formation of DD and 1-MBDD from the O_2 + M2 reaction.

BFRs, the preference of Br abstraction becomes practically relevant to the formation of PBDD/Fs.

It is worthwhile mentioning that, reactions of aromatic compounds with H/O radicals do not exhibit a general trend with regard to the importance of abstraction and addition channels. For example, addition channel dominates the overall reaction of OH with benzene, up to a temperature of 400 K.[57] In the system of benzene + HO_2,[58] addition channel remains the sole preferred corridor even at elevated temperatures. Experimental studies on pyrolysis of chlorobenzene[59] and chlorobiphenyls (PCBs)[60] revealed that, addition reactions in fact are more important than Cl abstraction reactions even at temperatures as high as 1000−1300 K. To gain further insight into the noticeable difference in the behavior between the H + PBDEs system studied herein and the experimental findings of dominance of addition channels in chlorinated aromatics, we have considered reactions of H + chlorobenzene and H + bromobenzene.

Reaction coordinates for the two systems are given in Figure S2 of the Supporting Information. Calculated reactions rate constants for addition and abstraction channels are listed in Table S2. Branching ratios for addition and abstraction channels for the two systems are plotted in Figure S3. It is evident that, the system of H + bromobenzene behaves similarly to the system H + PBDEs, in terms of the dominance of the abstraction channels at all temperatures. Our results for the system of H + chlorobenzene agree also with experimental findings on the importance of addition channels at high

dx.doi.org/10.1021/es305081j | Environ. Sci. Technol. 2013, 47, 5118−5127

temperatures. The difference in behavior between the H + chlorobenzene and H + bromobenzene stems from two factors. First, the system of H + bromobenzene entails very similar activation energies for addition and abstraction channels. In comparison, the activation energy for the addition channel in the system of H + chlorobenzene is noticeably smaller than that of the abstraction channel. Second, an entropic loss associated with removal of a species acts in favor of the abstraction channel in the system of H + bromobenzene. The large difference in activation energies between the two channels in the system of H + chlorobenzene counterbalances the effect of entropy change throughout low and intermediate temperature ranges.

Reaction with Triplet Ground State Oxygen Molecules. Reaction of closed-shell hydrocarbons with triplet ground-state oxygen molecules represents a highly endoergic process.[61] Consequently, most kinetic models on combustion of hydrocarbons excluded this reaction from their analyses even at low temperatures. Despite their considerable endoergicity, reactions involving triplet oxygen molecules with stable hydrocarbons could be important prior to the establishment of the reactive O/H radical pool. Direct abstraction of an H atom from a 2,2′-DBDE molecule by an oxygen molecule, and the formation of HO_2 radicals, is found to be vastly endoergic by 76.1 kcal/mol and highly unlikely to be of any significance. Alternatively, we found a triplet oxygen molecule to be capable of displacing a bromine atom and to form a peroxy-type radical (Scheme 1).

Endoergicity of this reaction is estimated to be 39.9 kcal/mol with a barrier height that it is only 1.6 kcal/mol higher, via the transition structure TS1, than the separated products. A rate constant for this Br-displacement reaction is fitted to $k(T) = 3.02 \times 10^{-23} T^{2.79} \exp(-19\,000/T)$ $cm^3 \cdot molecule^{-1} \cdot s^{-1}$ (per one available Br site). To assess the plausible significance of initial oxidation of 2,2′-DBDE by the triplet oxygen through displacement of a Br atom, a unimolecular-like rate constant is obtained by using atmospheric oxygen concentration at elevated temperatures (i.e., 1.92×10^{18} molecule/cm^3 at 800 K). The rate constants for unimolecular decomposition of 2,2′-DBDE molecule are compared with rate constants for bimolecular Br-displacement reactions in the decomposition of the 2,2′-DBDE molecule. It is found that, the rate of Br-displacement by the triplet oxygen competes with the rate of the direct unimolecular decomposition of the 2,2′-DBDE at all temperatures, viz., 3.53×10^{-7} s^{-1} versus 4.74×10^{-7} s^{-1} at 800 K. The rate constant for the reverse reaction is fitted to $k(T) = 6.30 \times 10^{-18} T^{1.88} \exp(-900/T)$ $cm^3 \cdot molecule^{-1} \cdot s^{-1}$. The importance of this reaction under conditions encountered in real combustion environment is two-fold. It provides a route for the initial oxidation of PBDEs in the absence of O/H radical pool and it releases the reactive bromine atoms.

Reaction with Br Atoms. The concentration of bromine atoms is typically lower than the concentration of chlorine atoms in combustion systems.[62] However, cocombustion of BFRs-treated materials in municipal waste incinerators could create a relatively bromine-rich environment.[33] The existence of free bromine atoms in the combustion atmosphere is evident from the formation of brominated/chlorinated dioxins, i.e., PXDD/Fs.[63,64] Bromine atoms could also be generated from Br_2, which arises in the combustion of Br-containing fuels, functioning as a brominating agent.[65] Metallic oxide catalysts could also act to release bromine atoms from BFRs attached to polymer backbones.[37,66]

Reaction of bromine atoms with 2,2′-DBDE molecules branches into three pathways as described in Figure 3. Formation of 1,2-dibromobenzene and 2-bromophenoxy, upon addition of Br at an edge of the ether bridge, demands a modest activation energy of 17.0 kcal/mol via the transition structure TS2_Br. This process liberates 8.1 kcal/mol of excess energy. The estimated reaction barrier is in a relative agreement with an empirical value derived by Wiater and Louw[67] of 19.0 kcal/mol. Abstractions of H and Br atoms are predicted to be endoergic by 23.7 and 28.1 kcal/mol, respectively. The latter requires overcoming a reaction barrier that is almost as high as the reaction energy, i.e., 23.9 kcal/mol. Branching ratios for the H abstraction channel (per one abstractable H atom) and Br addition at the pivot carbon atom are depicted in Figure 3, based on the calculated reaction rate constant given in Table 1. Breakage of the ether linkage contributes a branching fraction of between 0.18 and 0.08 in the temperature range of 600−1000 K. This observation is in accord with the findings of Wiater and Louw,[67] with regard to the relative rates of H abstraction and breakage of the ether linkage. Clearly, the overall importance of fission of the ether bridge further diminishes as the degree of bromination decreases. However, formation of hexabromobenzene and pentabromophenoxy is the sole channel for the reaction of Br with fully brominated PBDE, i.e., decaBDE. This reaction could explain the experimental observation that, hexabromobenzene and pentabromophenoxy constitute the dominant initial products of the slow pyrolysis of decaBDE.[54]

To conclude this section, OH reactions have been recently investigated experimentally[68] and theoretically[69,70] for various congeners of PBDEs. It has been found that, H abstractions represent the dominant channels at temperatures of relevance to the formation of PBDD/Fs from PBDEs (i.e., 600−1000 K), whereas the addition channels predominate at near-ambient temperature.

Formation of PBDFs. Considering the sizable energy requirements that characterize formation of PBDFs through direct elimination of HBr or Br_2, and formation of bromophenols/bromobenzenes through the breakage of the ether linkage, most plausible intermediates for the synthesis of PBDFs are phenyl-type radicals that form upon the facile H/Br abstraction from ortho positions in PBDEs. The top leftmost part of Figure 4 demonstrates pathways for the formation of 4-MCDF and dibenzofuran (DF) from the M2 intermediate that arises after the loss of an ortho Br atom from 2,2′-DBDE. The M2 intermediate initiates two ring-closure reactions. Attachment of the apparent radical site in M2 to the Br-substituted ortho position in the other phenyl ring occurs simultaneously with the departure of the bromine atom. The categorically exoergic formation of a DF molecule via this process necessitates a modest reaction barrier of 14.6 kcal/mol, as characterized by the transition structure TS3. Alternatively, the M3 intermediate could be formed by linking a radical site on one phenyl with the ortho carbon atom on the other phenyl, through a reaction barrier of 10.5 kcal/mol as marked by the transition structure TS2. The preference of ring closure involving an ortho hydrogen atom over that involving an ortho bromine atom originates from the nature of bromine atoms as electron-withdrawing groups. The increase in electron delocalization in the carbon *gem* to the Br atom in the ortho position and the voluminous size of Br atoms collaborate to increase the barrier associated with TS3 in comparison to that of TS2. Direct expulsion of the out-of-plane H atom in the M3

dx.doi.org/10.1021/es305081j | *Environ. Sci. Technol.* 2013, 47, 5118−5127

intermediate affords 4-MCDF through the transition structure TS4, characterized by a reaction barrier of 21.4 kcal/mol. Reaction rate constants for the two ring-closure reactions of M2 listed in Table 1 indicate competitive formation of DF and 4-MCDF. Larger entropy of activation for the reaction M2 → DF + Br counterbalances a lower energy of activation for the reaction M2 → M3 at intermediate temperatures. Formation of DF is predicted to contribute a fraction of 0.25−0.55 to the unimolecular isomerization of M2 in the temperature interval of 600−1000 K. It follows that, ring-closure reactions are not greatly influenced by the atomic type of the ortho substitution on the other phenyl ring.

Br atoms characterized by their long-range van der Waals radii at 1.901 Å could create a "steric crowding", which in turn may hinder ring-closure of highly brominated congeners of M2. To address this point, we investigate, in Figure S4 of the Supporting Information, ring-closure reactions for isomers of M2 with various bromination patterns that could exist in the vicinity of the ether linkage. Evidently, changes in degree and pattern of bromination have a rather minor influence on the activation energy of both categories of ring-closure reactions. Accordingly, a prerequisite to form PBDFs from PBDEs is the loss on an ortho atom regardless of the degree and pattern of bromination on either of the two phenyl rings. Practical relevance of this observation follows from the deployment of highly brominated congeners of PBDEs in commercial formulations of flame retardants.

Formation of PBDDs. Figure 4 elucidates detailed mechanisms of the formation of 1-MBDD and DD (dibenzo-*p*-dioxin) from the oxidation of a 2,2′-DBDE molecule. Energy differences between the various conformers are given in Figure 4. Oxidation of the M2 structure commences with the addition of an oxygen molecule to its radical center forming the peroxy-type radical of M1. This reaction proceeds without an intrinsic barrier with an estimated exoergicity of 43.4 kcal/mol. As discussed above, the M1 adduct could also result via Br displacement performed by a molecule of the ground-state triplet oxygen. Intermolecular arrangements and O−O bond scission predominate the fate of the M1 adduct. In an analogy to the well-established routes in the low-temperature oxidation of aromatics,[71,72] M1 intermediate isomerizes into the dioxiranyl-type radical (M8) and the 1,2-dioxetanyl-type radical (M6) requiring overcoming the reaction barriers of 25.6 (TS6) and 45.4 kcal/mol (TS7), respectively. Formation of M6 and M8 is predicted to be endoergic by 17.0 and 40.2 kcal/mol, correspondingly. Alternatively, the O−O bond fission costs 34.4 kcal/mol and creates the phenoxy-type radical of M7. Generally, M7 could also be sourced from the reaction sequence ROO + R′H → ROOH + R′ → RO + OH + R′ that often prevails in the low-temperature oxidation of hydrocarbons.[73] The M7 adduct undergoes two coupling reactions to form two dioxin products, DD and 1-MBDD. The transition structures TS13 and TS14 track the attachment of the phenoxy-O atom to Br- and H-substituted positions while climbing modest barriers of 27.4 and 24.3 kcal/mol, respectively. The difference between these two values follows from a weak repulsion between the two partially charged O and Br atoms. Nevertheless, reaction rate constants recorded in Table 1 suggest that, these two reactions compete for the formation of DD and 1-MBDD. The M7 adduct could also experience the so-called "ring contraction/CO elimination" reaction sequence as shown in the upper rightmost part of Figure 4. However, this operation should be inhibited by the soaring energy barrier of TS16 (55.4 kcal/mol) in reference to that of TS13 and TS14.

Formation of the M4 moiety is associated with the lowest energy barrier among all exit channels for the unimolecular decomposition of the M1 intermediate, as induced by the transition structure TS5. In TS5, the outer oxygen atom of the peroxyl group bridges over at the pivot carbon atom of the other phenyl ring through a barrier of 16.8 kcal/mol:

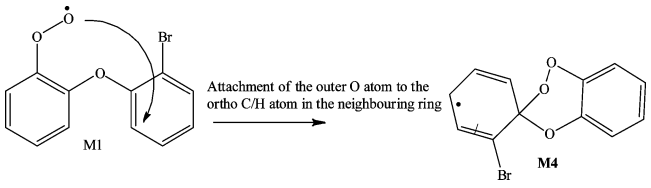

As evident from the reaction rate constants of Table 1, generation of the M4 intermediate should predominate the fate of the initial peroxy adduct of M1 at all temperatures. The M4 adduct functions as the intermediate for the product flux into dioxins. As shown in the middle of Figure 4, two oxirane-type structures (M5 and M17) evolve from the M4 intermediate along pathways of very comparable activation energies of 14.3 (TS8) and 15.4 kcal/mol (TS19):

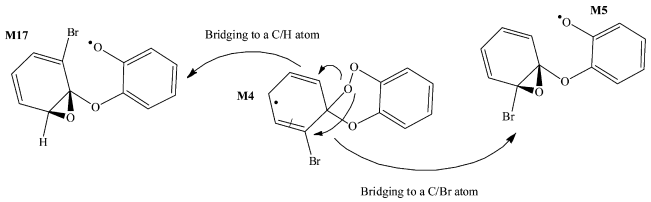

Consequently, formation of the two-membered ring structures is insensitive to the type of atoms at the ortho site (Br versus H), and the formation of the oxirane-type intermediate should also apply to more fully brominated congeners of M4.

A noticeable difference in barriers heights between TS9 and TS10 favors cyclization of M5 into M9 over intramolecular H shift to yield intermediate M11. The OH-1-MBDD (M10) intermediate forms upon H migration into the oxiranyl O atom via a reaction barrier of 28.9 kcal/mol (TS11) in an exoergic reaction of −28.0 kcal/mol. The loss of the out-of-plane weakly attached OH group in M10 liberates the 1-MBDD molecule:

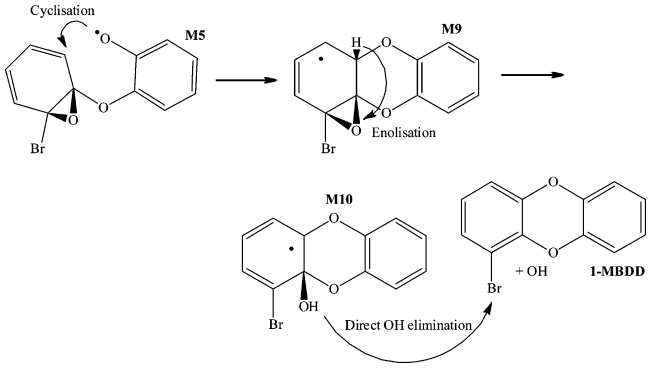

In an analogy, cyclization of M17 moiety affords the oxirane-type structure of M18 and subsequently the M19 intermediate following the loss of a Br atom. Direct expulsion of the oxiranyl O atom in M19 is a spin-forbidden process. Alternatively, bimolecular reactions of the M19 moiety with reactive radicals (X) is more practicable and results in the formation of an OX-

dx.doi.org/10.1021/es305081j | Environ. Sci. Technol. 2013, 47, 5118−5127

DD structure. For instance, bimolecular reaction of M19 with Br atoms proceeds via a modest reaction barrier of 15.0 kcal/mol (TS21) to form the OBr-DD structure of M20. Departure of the OBr moiety in the M20 structure occurs through a trivial barrier of 11.9 kcal/mol and produces a DD molecule.

Figure 5 shows the energetics of the formation of DD and 1-MCDD in reference to the separated initial reactants, i.e., an oxygen molecule and the M2 intermediate. As demonstrated in Figure 5, the final products of the reaction of 1-MCDD and the propagating radical OH reside in a well-depth of 77.1 kcal/mol in reference to the separated reactants. The overall reaction barrier is remarkably shallower, by 11.6 kcal/mol, than the separated reactants (TS12). Formation of OBr and DD also exhibits similar exoergic trends. Overall, a loss of an ortho atom from PBDEs represents a bottleneck for the generation of dioxins. Subsequent steps in the direction of dioxins' formation following the appearance of an ortho-centered radical of PBDEs are rather facile. The energetic trend in Figure 5 clearly accounts for the formation of appreciable concentrations of PBDD/Fs from oxidation of PBDEs.

■ ASSOCIATED CONTENT

Ⓢ Supporting Information

Cartesian coordinates, total energies and vibrational frequencies for all structures; NASA polynomial coefficients for all structures; and a PES figure for formation of PBDFs from different brominated isomers of PBDEs. This material is available free of charge via the Internet at http://pubs.acs.org.

■ AUTHOR INFORMATION

Corresponding Author

*E-mail: Mohammednoor.Altarawneh@newcastle.edu.au; Tel: (+61) 2 4985-4286.

Present Address

†Also at Chemical Engineering Department, Al-Hussein Bin Talal University, Ma'an, Jordan

Notes

The authors declare no competing financial interest.

■ ACKNOWLEDGMENTS

This study has been supported by a grant of computing time from the National Computational Infrastructure (NCI), Australia (Project ID: De3) as well as funds from the Australian Research Council (ARC) and Faculty of Engineering and Built Environment at the University of Newcastle, Australia.

■ REFERENCES

(1) Alaee, M.; Arias, P.; Sjödin, A.; Bergman, Å. An overview of commercially used brominated flame retardants, their applications, their use patterns in different countries/regions and possible modes of release. *Environ. Int.* **2003**, *29*, 683−689.

(2) Weber, L. W. D.; Greim, H. The toxicity of brominated and mixed-halogenated dibenzo-*p*-dioxins and dibenzofurans: An overview. *J. Toxicol. Environ. Health* **1997**, *50*, 195−215.

(3) McDonald, T. A. A perspective on the potential health risks of PBDEs. *Chemosphere* **2002**, *46*, 745−755.

(4) Alaee, M. Recent progress in understanding of the levels, trends, fate and effects of BFRs in the environment. *Chemosphere* **2006**, *64*, 179−180.

(5) Law, R. J.; Herzke, D.; Harrad, S.; Morris, S.; Bersuder, P.; Allchin, C. R. Levels and trends of HBCD and BDEs in the European and Asian environments, with some information for other BFRs. *Chemosphere* **2008**, *73*, 223−241.

(6) Siddiqi, M. A.; Laessig, R. H.; Reed, K. D. Polybrominated diphenyl ethers (PBDEs): New pollutants-old diseases. *Clin. Med. Res.* **2003**, *1*, 281−290.

(7) Ali, N.; Harrad, S.; Goosey, E.; Neels, H.; Covaci, A. "Novel" brominated flame retardants in Belgian and UK indoor dust: Implications for human exposure. *Chemosphere* **2011**, *83*, 1360−1365.

(8) Gaylor, M. O.; Harvey, E.; Hale, R. C. House crickets can accumulate polybrominated diphenyl ethers (PBDEs) directly from polyurethane foam common in consumer products. *Chemosphere* **2012**, *86*, 500−505.

(9) Barontini, F.; Marsanich, K.; Petarca, L.; Cozzani, V. Thermal degradation and decomposition products of electronic boards containing BFRs. *Ind. Eng. Chem. Res.* **2005**, *44*, 4186−4199.

(10) Yang, X.; Sun, L.; Xiang, J.; Hu, S.; Su, S. Pyrolysis and dehalogenation of plastics from waste electrical and electronic equipment (WEEE): A review. *Waste Manage. (Amsterdam, Neth.)*.

(11) Consonni, S.; Viganò, F. Material and energy recovery in integrated waste management systems: The potential for energy recovery. *Waste Manage. (Amsterdam, Neth.)* **2011**, *31*, 2074−2084.

(12) Wang, J.; Ma, Y.-J.; Chen, S.-J.; Tian, M.; Luo, X.-J.; Mai, B.-X. Brominated flame retardants in house dust from e-waste recycling and urban areas in South China: Implications on human exposure. *Environ. Int.* **2010**, *36*, 535−541.

(13) Van den Berg, M. B.; Birnbaum, L. S.; Denison, M.; De Vito, M.; Farland, W.; Feeley, M.; Fiedler, H.; Hakansson, H.; Hanberg, A.; Haws, L.; Rose, M.; Safe, S.; Schrenk, D.; Tohyama, C.; Tritscher, A.; Tuomisto, J.; Tysklind, M.; Walker, N.; Peterson, R. E. The 2005 World health organization reevaluation of human and mammalian toxic equivalency factors for dioxins and dioxin-like compounds. *Toxicol. Sci.* **2006**, *93*, 223−241.

(14) Samara, F.; Wyrzykowska, B.; Tabor, D.; Touati, D.; Gullett, B. K. Toxicity comparison of chlorinated and brominated dibenzo-*p*-dioxins and dibenzofurans in industrial source samples by HRGC/HRMS and enzyme immunoassay. *Environ. Int.* **2010**, *36*, 247−253.

(15) Hansson, S. O. Regulating BFRs − From science to policy. *Chemosphere* **2008**, *73*, 144−147.

(16) United Nations, *Stockholm Convention on Persistent Organic Pollutants, Adoption of Amendments to Annexes a, b and c*; Stockholm, 2009.

(17) Brominated Science and Environmental Forum (BSEF). http://www.bsef.com/regulation/ (accessed Nov 2012).

(18) Söderström, G.; Marklund, S. PBCDD and PBCDF from incineration of waste-containing brominated flame retardants. *Environ. Sci. Technol.* **2002**, *36*, 1959−1964.

(19) Söderström, G.; Marklund, S. Formation of PBCDD and PBCDF during flue gas cooling. *Environ. Sci. Technol.* **2003**, *38*, 825−830.

(20) Wang, L.-C.; Chang-Chien, G.-P. Characterizing the emissions of polybrominated dibenzo-*p*-dioxins and dibenzofurans from municipal and industrial waste incinerators. *Environ. Sci. Technol.* **2007**, *41*, 1159−1165.

(21) Wang, L.-C.; Wang, Y.-F.; Hsi, H.-C.; Chang-Chien, G.-P. Characterizing the emissions of polybrominated diphenyl ethers (PBDEs) and polybrominated dibenzo-*p*-dioxins and dibenzofurans (PBDD/Fs) from metallurgical processes. *Environ. Sci. Technol.* **2010**, *44*, 1240−1246.

(22) Sakai, S.-i.; Watanabe, J.; Honda, Y.; Takatsuki, H.; Aoki, I.; Futamatsu, M.; Shiozaki, K. Combustion of brominated flame retardants and behavior of its byproducts. *Chemosphere* **2001**, *42*, 519−531.

(23) Duan, H.; Li, J.; Liu, Y.; Yamazaki, N.; Jiang, W. Characterization and inventory of PCDD/Fs and PBDD/Fs emissions from the incineration of waste printed circuit board. *Environ. Sci. Technol.* **2011**, *45*, 6322−6328.

(24) Schüler, D.; Jager, J. Formation of chlorinated and brominated dioxins and other organohalogen compounds at the pilot incineration plant VERONA. *Chemosphere* **2004**, *54*, 49−59.

(25) Buser, H. R. Polybrominated dibenzofurans and dibenzo-*p*-dioxins: Thermal reaction products of polybrominated diphenyl ether flame retardants. *Environ. Sci. Technol.* **1986**, *20*, 404−408.
(26) Dumler, R.; Lenoir, D.; Thoma, H.; Hutzinger, O. Thermal formation of polybrominated dibenzofurans and dioxins from decabromodiphenyl ether flame retardant: Influence of antimony(III) oxide and the polymer matrix. *Chemosphere* **1990**, *20*, 1867−1873.
(27) Dumler, R.; Thoma, H.; Lenoir, D.; Hutzinger, O. PBDF and PBDD from the combustion of bromine containing flame retarded polymers: A survey. *Chemosphere* **1989**, *19*, 2023−2031.
(28) Dumler, R.; Thoma, H.; Lenoir, D.; Hutzinger, O. Thermal formation of polybrominated dibenzodioxins (PBDD) and dibenzofurans (PBDF) from bromine containing flame retardants. *Chemosphere* **1989**, *19*, 305−308.
(29) Thoma, H. Pcdd/F-concentrations in chimney soot from house heating systems. *Chemosphere* **1988**, *17*, 1369−1379.
(30) Thoma, H.; Hauschulz, G.; Hutzinger, O. Chlorine-bromine exchange during pyrolysis of 1,2,3,4-tetrabromodibenzodioxin with various chlorine donors. *Chemosphere* **1987**, *16*, 1579−1581.
(31) Wang, L.-C.; Hsi, H.-C.; Wang, Y.-F.; Lin, S.-L.; Chang-Chien, G.-P. Distribution of polybrominated diphenyl ethers (PBDEs) and polybrominated dibenzo-*p*-dioxins and dibenzofurans (PBDD/Fs) in municipal solid waste incinerators. *Environ. Pollut.* **2010**, *158*, 1595−1602.
(32) Altarawneh, M.; Dlugogorski, B. Z.; Kennedy, E. M.; Mackie, J. C. Mechanisms for formation, chlorination, dechlorination and destruction of polychlorinated dibenzo-*p*-dioxins and dibenzofurans (PCDD/Fs). *Prog. Energy. Combust. Sci* **2009**, *35*, 245−274.
(33) Weber, R.; Kuch, B. Relevance of BFRs and thermal conditions on the formation pathways of brominated and brominated−chlorinated dibenzodioxins and dibenzofurans. *Environ. Int.* **2003**, *29*, 699−710.
(34) Buser, H. R. Selective detection of brominated aromatic compounds using gas chromatography/negative chemical ionization mass spectrometry. *Anal. Chem.* **1986**, *58*, 2913−2919.
(35) Cao, H.; He, M.; Sun, Y.; Han, D. Mechanical and kinetic studies of the formation of polyhalogenated dibenzo-*p*-dioxins from hydroxylated polybrominated diphenyl ethers and chlorinated derivatives. *J. Phys. Chem. A* **2011**, *115*, 13489−13497.
(36) Erickson, P. R.; Grandbois, M.; Arnold, W. A.; McNeill, K. Photochemical formation of brominated dioxins and other products of concern from hydroxylated polybrominated diphenyl ethers (OH-PBDEs). *Environ. Sci. Technol.* **2012**, *46*, 8174−8180.
(37) Lenoir, D.; Zier, B.; Bieniek, D.; Kettrup, A. The influence of water and metals on PBDD/F concentration in incineration of decabrombiphenyl ether in polymeric matrices. *Chemosphere* **1994**, *28*, 1921−1928.
(38) Haglund, P. On the identity and formation routes of environmentally abundant tri- and tetrabromodibenzo-*p*-dioxins. *Chemosphere* **2010**, *78*, 724−730.
(39) Evans, C. S.; Dellinger, B. Mechanisms of dioxin formation from the high-temperature pyrolysis of 2-Bromophenol. *Environ. Sci. Technol.* **2003**, *37*, 5574−5580.
(40) Evans, C. S.; Dellinger, B. Mechanisms of dioxin formation from the high-temperature oxidation of 2-bromophenol. *Environ. Sci. Technol.* **2005**, *39*, 2128−2134.
(41) Evans, C. S.; Dellinger, B. Formation of bromochlorodibenzo-*p*-dioxins and dibenzofurans from the high-temperature oxidation of a mixture of 2-chlorophenol and 2-bromophenol. *Environ. Sci. Technol.* **2006**, *40*, 3036−3042.
(42) Yu, W.; Hu, J.; Xu, F.; Sun, X.; Gao, R.; Zhang, Q.; Wang, W. Mechanism and direct kinetics study on the homogeneous gas-phase formation of PBDD/Fs from 2-BP, 2,4-DBP, and 2,4,6-TBP as precursors. *Environ. Sci. Technol.* **2011**, *45*, 1917−1925.
(43) Frisch, M. J.; Trucks, G. W.; Schlegel, H. B.; Scuseria, G. E.; Robb, M. A.; Cheeseman, J. R.; Scalmani, G.; Barone, V.; Mennucci, B.; Petersson, G. A.; Nakatsuji, H.; Caricato, M.; Li, X.; Hratchian, H. P.; Izmaylov, A. F.; Bloino, J.; Zheng, G.; Sonnenberg, J. L.; Hada, M.; Ehara, M.; Toyota, K.; Fukuda, R.; Hasegawa, J.; Ishida, M.; Nakajima, T.; Honda, Y.; Kitao, O.; Nakai, H.; Vreven, T.; Montgomery, J. A., Jr.; Peralta, J. E.; Ogliaro, F.; Bearpark, M.; Heyd, J. J.; Brothers, E.; Kudin, K. N.; Staroverov, V. N.; Kobayashi, R.; Normand, J.; Raghavachari, K.; Rendell, A.; Burant, J. C.; Iyengar, S. S.; Tomasi, J.; Cossi, M.; Rega, N.; Millam, J. M.; Klene, M.; Knox, J. E.; Cross, J. B.; Bakken, V.; Adamo, C.; Jaramillo, J.; Gomperts, R.; Stratmann, R. E.; Yazyev, O.; Austin, A. J.; Cammi, R.; Pomelli, C.; Ochterski, J. W.; Martin, R. L.; Morokuma, K.; Zakrzewski, V. G.; Voth, G. A.; Salvador, P.; Dannenberg, J. J.; Dapprich, S.; Daniels, A. D.; Farkas, Ö.; Foresman, J. B.; Ortiz, J. V.; Cioslowski, J.; Fox, D. J. *Gaussian 09*, A.1; Gaussian, Inc: Wallingford, CT, 2009.
(44) Zhao, Y.; Schultz, N. E.; Truhlar, D. G. Design of density functionals by combining the method of constraint satisfaction with parametrization for thermochemistry, thermochemical kinetics, and noncovalent interactions. *J. Chem. Theory Comput.* **2006**, *2*, 364−382.
(45) Montgomery, J. J. A.; Ochterski, J. W.; Petersson, G. A. A complete basis set model chemistry. IV. An improved atomic pair natural orbital method. *J. Chem. Phys.* **1994**, *101*, 5900−5909.
(46) Wheeler, S. E.; Houk, K. N. Integration grid errors for meta-GGA-predicted reaction energies: Origin of grid errors for the M06 suite of functionals. *J. Chem. Theory Comput* **2010**, *6*, 395−404.
(47) Mokrushin, V. B.; Bedanov, V.; Tsang, W.; Zachariah, M.; Knyazev, V *ChemRate*, V.1.19; NIST: Gaithersburg, MD, 2002.
(48) Wigner, E. On the quantum correction for thermodynamic equilibrium. *Phys. Rev.* **1932**, *40*, 749−759.
(49) Oyola, Y.; Singleton, D. A. Dynamics and the failure of transition state theory in alkene hydroboration. *J. Am. Chem. Soc.* **2009**, *131*, 3130−3131.
(50) Doubleday, C.; Suhrada, C. P.; Houk, K. N. Dynamics of the degenerate rearrangement of bicyclo[3.1.0]hex-2-ene. *J. Am. Chem. Soc.* **2005**, *128*, 90−94.
(51) Burcat, A. Thermochemical Data for Combustion Calculations. Chapter 8 In *Combustion Chemistry*, Gardiner, W. C., Ed. Springer-Verlag: New York, NY, 1984.
(52) Rao, V. S.; Skinner, G. B. Formation of hydrogen and deuterium atoms in the pyrolysis of toluene-d_8 and toluene-α,α,α-d_3 behind shock waves. *J. Phys. Chem.* **1989**, *93*, 1864−1869.
(53) van Scheppingen, W.; Dorrestijn, E.; Arends, I.; Mulder, P.; Korth, H.-G. Carbon−oxygen bond strength in diphenyl ether and phenyl vinyl ether: An experimental and computational study. *J. Phys. Chem. A* **1997**, *101*, 5404−5411.
(54) Danzer, B.; Riess, M.; Thoma, H.; Vierle, O.; van Eldik, R. Pyrolysis of plastic containing flame retardants. *Organohalogen Compd.* **1997**, *31*, 108−113.
(55) Luijk, R.; Govers, H. A. J. The formation of polybrominated dibenzo-*p*-dioxins (PBDDs) and dibenzofurans (PBDFs) during pyrolysis of polymer blends containing brominated flame retardants. *Chemosphere* **1992**, *25*, 361−374.
(56) Luijk, R.; Wever, H.; Olie, K.; Govers, H. A. J.; Boon, J. J. The influence of the polymer matrix on the formation of polybrominated dibenzo-*p*-dioxins (PBDDs) and polybrominated dibenzofurans (PBDFs). *Chemosphere* **1991**, *23*, 1173−1183.
(57) Chen, C.-C.; Bozzelli, J. W.; Farrell, J. T. Thermochemical properties, pathway, and kinetic analysis on the reactions of benzene with OH: An elementary reaction mechanism. *J. Phys. Chem. A* **2004**, *108*, 4632−4652.
(58) Altarawneh, M.; Dlugogorski, B. Z.; Kennedy, E. M.; Mackie, J. C. Theoretical study of reactions of HO_2 in low-temperature oxidation of benzene. *Combust. Flame* **2010**, *157*, 1325−1330.
(59) Ritter, E. R.; Bozzelli, J. W.; Dean, A. M. Kinetic study on thermal decomposition of chlorobenzene diluted in H_2. *J. Phys. Chem.* **1990**, *94*, 2493−2504.
(60) Manion, J. A.; Mulder, P.; Louw, R. Gas-phase hydrogenolysis of polychlorobiphenyls. *Environ. Sci. Technol.* **1985**, *19*, 280−282.
(61) Altarawneh, M. K.; Dlugogorski, B. Z.; Kennedy, E. M.; Mackie, J. C. Rate constants for reactions of ethylbenzene with hydroperoxyl radical. *Combust. Flame* **2013**, *160*, 9−16.
(62) Vainikka, P.; Hupa, M. Review on bromine in solid fuels − Part 2: Anthropogenic occurrence. *Fuel* **2012**, *94*, 34−51.

(63) Du, B.; Zheng, M.; Huang, Y.; Liu, A.; Tian, H.; Li, L.; Li, N.; Ba, T.; Li, Y.; Dong, S.; Liu, W.; Su, G. Mixed polybrominated/chlorinated dibenzo-*p*-dioxins and dibenzofurans in stack gas emissions from industrial thermal processes. *Environ. Sci. Technol.* **2010**, *44*, 5818−5823.
(64) Kawamoto, K. Potential formation of PCDD/Fs and related bromine-substituted compounds from heating processes for ashes. *J. Hazard. Mater.* **2009**, *168*, 641−648.
(65) Kanters, J.; Louw, R. Thermal and catalysed halogenation in combustion reactions. *Chemosphere* **1996**, *32*, 89−97.
(66) Luijk, R.; Dorland, C.; Smit, P.; Jansen, J.; Govers, H. A. J. The role of bromine in the de novo synthesis in a model fly ash system. *Chemosphere* **1994**, *28*, 1299−1309.
(67) Wiater, I.; Louw, R. Reactions of diphenyl ether with chlorine and bromine atoms around 750 K − Relevance for gas-phase "dioxin" formation. *Eur. J. Org. Chem.* **1999**, *1999*, 261−265.
(68) Raff, J. D.; Hites, R. A. Gas-phase reactions of brominated diphenyl ethers with OH radicals. *J. Phys. Chem. A* **2006**, *110*, 10783−10792.
(69) Cao, H.; He, M.; Han, D.; Sun, Y.; Xie, J. Theoretical study on the mechanism and kinetics of the reaction of 2,2′,4,4′-tetrabrominated diphenyl ether (BDE-47) with OH radicals. *Atmos. Environ.* **2011**, *45*, 1525−1531.
(70) Cao, H.; He, M.; Han, D.; Sun, Y.; Zhao, S.; Ma, H.; Yao, S. Mechanistic and kinetic study on the reaction of 2,4-dibrominated diphenyl ether (BDE-7) with OH radicals. *Comput. Theor. Chem* **2012**, *983*, 31−37.
(71) Fadden, M. J.; Barckholtz, C.; Hadad, C. M. Computational study of the unimolecular decomposition pathways of phenylperoxy radical. *J. Phys. Chem. A* **2000**, *104*, 3004−3011.
(72) Altarawneh, M.; Dlugogorski, B. Z.; Kennedy, E. M.; Mackie, J. C. Quantum chemical study of low temperature oxidation mechanism of dibenzofuran. *J. Phys. Chem. A* **2006**, *110*, 13560−13567.
(73) Battin-Leclerc, F. Detailed chemical kinetic models for the low-temperature combustion of hydrocarbons with application to gasoline and diesel fuel surrogates. *Prog. Energy Combust. Sci.* **2008**, *34*, 440−498.